Research Square

Preprints are preliminary reports that have not undergone peer review.
They should not be considered conclusive, used to inform clinical practice,
or referenced by the media as validated information.

METTL15-mediated m4C modification regulates glucose metabolic reprogramming in a c-Myc translation-dependent manner and promotes hepatocellular carcinoma progression

Longhui Xie
The Central Hospital
Zhengsheng Ouyang
YongZhou Vocational Technical College
Changbin Pan
The Central Hospital
Lijuan Lv
The Central Hospital
Shaofei Xiao
The Central Hospital
Jining Zeng
The Central Hospital
Yang Yang
yydorispps@163.com

Department of Oncology,The Central Hospital of Shaoyang

Research Article

Keywords:

Posted Date: November 2nd, 2026

DOI: https://doi.org/10.21203/rs.3.rs-8062434/v1

License: This work is licensed under a Creative Commons Attribution 4.0 International License.
Read Full License

Additional Declarations: No competing interests reported.

METTL15-mediated m^4C modification regulates glucose metabolic reprogramming in a c-Myc translation-dependent manner and promotes hepatocellular carcinoma progression

Longhui Xie[1,2#], Zhengsheng Ouyang[4#], Changbin Pan[1,2#], Lijuan Lv[1,2], Shaofei Xiao[1,2], Jining Zeng[1,2], Yang Yang[3*]

[1] Department of Hepatobiliary Pancreatic Spleen Surgery, The Central Hospital of ,Yongzhou, China

[2] Department of Hepatobiliary Pancreatic Spleen Surgery, Yongzhou Hospital Affiliated to University of South China, China

[3] Department of Oncology, The Central Hospital of Shaoyang,Shaoyang，422000，P.R. China

[4] Department of clinical medicine, YongZhou Vocational Technical College, Yongzhou, 425000, China.

[#]These authors contributed equally: Longhui Xie, Zhengsheng Ouyang, Changbin Pan.

Correspondence

Yang Yang , M.D. E-mail: yydorispps@163.com

Abstract

HCC is a highly aggressive malignancy with limited treatment options and poor prognosis. Metabolic reprogramming, particularly enhanced glycolysis, is a hallmark of HCC progression, yet the underlying regulatory mechanisms remain incompletely understood. METTL15, a m^4C RNA methyltransferase, has recently been implicated in mitochondrial function, but its role in HCC is largely unknown. In this study, we reveal that METTL15 is significantly upregulated in HCC tissues and cell lines, and its high expression correlates with unfavorable clinical outcomes. Functional assays demonstrate that METTL15 promotes HCC cell proliferation, migration, and invasion, both in *vitro* and in *vivo*. Mechanistically, METTL15 enhances glycolytic flux by facilitating the translation of the oncogene c-Myc in an m^4C-dependent manner, thereby driving glucose metabolic reprogramming. Knockout of METTL15 suppresses glycolysis and attenuates c-Myc protein expression without affecting its mRNA levels, suggesting a post-transcriptional regulatory axis. Our findings identify METTL15 as a novel epitranscriptomic regulator of glucose metabolism in HCC and highlight its potential as a promising therapeutic target.

Keywords： m^4C, translational regulation, glycolysis, hepatocellular carcinoma, RNA modification, tumor progression

Introduction

Hepatocellular carcinoma (HCC) is one of the most common and aggressive malignancies worldwide, ranking as the third leading cause of cancer-related deaths[1, 2]. Despite recent advances in imaging-based screening, targeted therapies, and immunotherapy, the overall prognosis for HCC patients remains poor[1, 3]. This is largely due to the tumor's high metastatic potential, frequent postoperative recurrence, and resistance to conventional therapies[4]. In recent years, metabolic reprogramming, particularly the alteration of glucose metabolism has emerged as a hallmark of tumor development and progression[4, 5].

HCC cells tend to rely on enhanced glycolysis to meet their increased energy demands and biosynthetic needs during rapid proliferation[6-11]. Notably, they preferentially metabolize glucose to lactate even under aerobic conditions, a phenomenon known as the Warburg effect[12]. This form of aerobic glycolysis not only provides ATP but also generates intermediates for the synthesis of nucleotides, amino acids, and lipids[13]. In addition, glycolytic by-products such as lactate contribute to an immunosuppressive tumor microenvironment, angiogenesis, and metastasis. Therefore, targeting key enzymes in the glycolytic pathway, such as hexokinase 2 (HK2), pyruvate kinase M2 (PKM2), and lactate dehydrogenase A (LDHA) has become an emerging strategy for antitumor metabolic therapy[14-20].

RNA modifications have recently garnered attention as critical post-transcriptional regulators of gene expression and cellular metabolism[21-28]. Among these, N4-methylcytidine (m^4C) is a post-transcriptional modification predominantly found in

mitochondrial ribosomal RNA, catalyzed by the methyltransferase METTL15[29]. Previous studies have shown that METTL15-mediated m^4C methylation is essential for mitochondrial translation and the maintenance of oxidative phosphorylation homeostasis[30]. Whether METTL15 plays a role in metabolic reprogramming, especially glycolysis, in HCC remains largely unknown.

In our preliminary studies, we observed a significant upregulation of METTL15 in HCC cell lines and clinical tumor tissues[25], which was strongly associated with poor prognosis[22]. Functional experiments demonstrated that METTL15 knockout suppressed HCC cell proliferation and migration, accompanied by reduced glucose uptake and lactate production[4, 31, 32], suggesting a potential role in promoting tumor glycolysis. Mechanistically, we found that METTL15 regulates the translation of c-Myc, a master transcription factor known to activate the expression of multiple glycolytic enzymes and drive metabolic reprogramming in cancer cells[33, 34].

Therefore, this study aims to systematically investigate the oncogenic role of METTL15 and its involvement in glycolytic regulation in HCC. We comprehensively examine the expression pattern and clinical significance of METTL15, evaluate its impact on glycolytic activity and malignant behavior in *vitro* and in *vivo*, and further explore how METTL15 modulates c-Myc translation to facilitate glucose metabolic reprogramming[35, 36]. Through this work, we aim to deepen the understanding of RNA modification-mediated metabolic regulation in HCC and highlight METTL15 as a potential therapeutic target for metabolic intervention.

Materials and Methods

GEO and TCGA Data Acquisition and Analysis

Transcriptomic data and corresponding clinical information were retrieved from The Cancer Genome Atlas (TCGA) Liver Hepatocellular Carcinoma (LIHC) dataset (https://portal.gdc.cancer.gov/) and the Gene Expression Omnibus (GEO) database (https://www.ncbi.nlm.nih.gov/geo/). For TCGA-LIHC, RNA-sequencing data (HTSeq-FPKM format) and clinical annotations of 374 HCC tissues and 50 adjacent normal tissues were downloaded. GEO datasets including GSE14520 and GSE76427 were selected for validation based on sample size, data quality, and the availability of clinical metadata.

Differentially expressed genes (DEGs) between tumor and normal samples were identified using the “limma” or “DESeq2” R package, depending on the dataset format. Genes with an adjusted p-value < 0.05 and $|\log2 \text{ fold change}| > 1$ were considered statistically significant. Kaplan-Meier survival analysis was conducted using the “survival” and “survminer” R packages to assess the prognostic value of candidate genes. The expression patterns and prognostic relevance of METTL15 were visualized using boxplots and Kaplan-Meier curves, respectively. All analyses were performed using R software (version 4.2.2), and data preprocessing steps included background correction, log2 transformation, and batch effect adjustment where applicable.

Clinical Samples and Cell Culture

To further validate the bioinformatics findings, we collected tumor tissues and corresponding adjacent non-tumor tissues from clinically diagnosed hepatocellular

carcinoma (HCC) patients who underwent surgical resection at Yongzhou Central Hospital. All patients provided written informed consent, and the study was approved by the Institutional Ethics Committee of Yongzhou Central Hospital. All tissue specimens were immediately snap-frozen in liquid nitrogen and stored at -80 °C for subsequent RNA and protein extraction.

Human HCC cell lines (Hep3B, Huh7, and PLC/PRF/5) and normal liver epithelial cells (THLE-2) were obtained from the Cell Bank of the Chinese Academy of Sciences (Shanghai, China). Cells were cultured in Dulbecco's Modified Eagle Medium (DMEM, Gibco, USA) supplemented with 10% fetal bovine serum (FBS, Gibco, USA), 100 U/mL penicillin, and 100 μg/mL streptomycin. All cells were maintained in a humidified incubator at 37 °C with 5% CO_2. Cell line authentication was regularly confirmed by short tandem repeat (STR) profiling, and mycoplasma contamination was routinely tested.

RNA Extraction and Quantitative Real-Time PCR (qRT-PCR)

Total RNA was extracted from tissues and cultured cells using TRIzol reagent (R0016, Solarbio, China) according to the manufacturers instructions. The concentration and purity of RNA were determined using a NanoDrop 2000 spectrophotometer (Thermo Fisher Scientific, USA). RNA samples with an A260/A280 ratio between 1.8 and 2.0 were considered suitable for further analysis. For reverse transcription, 1 μg of total RNA was used to synthesize cDNA using the First Strand cDNA Synthesis Kit (R312, Solarbio, China). Quantitative real-time PCR was performed using 2× RealStar Green Fast Mixture (FP209, Solarbio, China) on a LightCycler® 480 System (Roche,

Switzerland). The PCR cycling conditions were as follows: initial denaturation at 95 °C for 30 s, followed by 40 cycles of 95 °C for 5 s and 60 °C for 30 s. Gene expression levels were normalized to GAPDH, and relative expression was calculated using the $2^{-\Delta\Delta ct}$ method. All experiments were performed in triplicate.

Western Blot Analysis

Total protein was extracted from cultured cells or tissue samples using RIPA lysis buffer (Solarbio, China) on ice for 30 minutes, followed by centrifugation at 12,000 rpm for 15 minutes at 4 °C. The supernatant was collected, and protein concentrations were determined using the BCA Protein Assay Kit (Solarbio, China). Equal amounts of protein (20-40 μg) were mixed with loading buffer, denatured at 95 °C for 5 minutes, and separated by SDS-PAGE. Proteins were then transferred onto PVDF membranes (Millipore, USA) using wet transfer at 300 mA for 1.5 hours under cooling conditions. Membranes were blocked in 5% non-fat milk for 1 hour at room temperature and incubated overnight at 4 °C with primary antibodies against specific proteins (e.g., METTL15, c-myc, HK2, PKM2, β-actin). The next day, membranes were washed with TBST (0.1% Tween-20 in TBS) three times and incubated with HRP-conjugated secondary antibodies (Solarbio, China) for 1 hour at room temperature. Signals were detected using enhanced chemiluminescence (ECL) reagent (Solarbio, China) and visualized with a chemiluminescence imaging system (Tanon, China). Band intensities were semi-quantitatively analyzed using ImageJ software, with GAPDH used as the internal loading control.

Immunohistochemistry (IHC)

Paraffin-embedded human or mouse liver tissue sections (4 μm thick) were subjected to immunohistochemical staining to evaluate protein expression. Briefly, tissue sections were deparaffinized in xylene and rehydrated through graded ethanol series. Antigen retrieval was performed by heating the slides in citrate buffer (pH 6.0) at 95 °C for 20 minutes. Endogenous peroxidase activity was blocked by incubation with 3% hydrogen peroxide for 10 minutes at room temperature. After washing with phosphate-buffered saline (PBS), the sections were blocked with 5% bovine serum albumin (BSA) for 30 minutes and then incubated overnight at 4 °C with primary antibodies against target proteins (METTL15, Ki-67, HK2, PKM2). The following day, slides were washed and incubated with HRP-conjugated secondary antibodies for 1 hour at room temperature. Color development was performed using 3,3′-diaminobenzidine (DAB) substrate solution (Solarbio, China), followed by hematoxylin counterstaining. Stained sections were dehydrated, cleared, and mounted with coverslips. Images were captured using a light microscope (Nikon, Japan). The intensity and percentage of positive staining were semi-quantitatively scored by two independent pathologists in a blinded manner.

METTL15 Overexpression and Knockout

To generate METTL15-overexpressing cells, the full-length coding sequence of human METTL15 was cloned into the pcDNA3.1 expression vector (Invitrogen, USA). HCC cells (e.g., Hep3B or Huh7) were transfected with the recombinant plasmid using Lipofectamine 3000 (Invitrogen, USA) according to the manufacturer's instructions. Stable overexpressing cell lines were selected using G418 (600 μg/mL) and validated by qRT-PCR and Western blot analysis.

For METTL15 knockout, a CRISPR/Cas9-based gene editing approach was employed. Single guide RNAs (sgRNAs) targeting exonic regions of the METTL15 gene were designed using an online tool (e.g., CRISPR Design Tool, MIT) and cloned into the lentiCRISPR v2 vector (Addgene #52961). Lentiviral particles were produced by co-transfecting the lentiCRISPR-sgMETTL15 vector with packaging plasmids (psPAX2 and pMD2.G) into HEK293T cells using Lipofectamine 3000. After 48-72 hours, viral supernatants were collected and used to infect HCC cells in the presence of polybrene (8 μg/mL). Puromycin (2 μg/mL) was used for stable selection. Successful knockout was confirmed by genomic PCR, qRT-PCR, and Western blot. A non-targeting sgRNA was used as a negative control. All constructs were verified by Sanger sequencing prior to transduction.

In *Vivo* Tumor Xenograft and Lung Metastasis Models

All animal experiments were approved by the Animal Care and Use Committee of Yongzhou Central Hospital and conducted in accordance with institutional guidelines and the Declaration of Helsinki. For the subcutaneous xenograft model, 4 to 6-week-old male BALB/c nude mice (purchased from Beijing Vital River Laboratory Animal Technology, China) were randomly divided into groups (n = 5 per group). HCC cells stably transfected with control vector, METTL15 overexpression, or METTL15 knockout constructs (5×10^6 cells in 100 μL PBS) were subcutaneously injected into the right axilla of each mouse. Tumor size was measured every 3 days using a digital caliper, and tumor volume was calculated using the formula: Volume = (Length × Width^2) / 2. On day 15 post-injection, the mice were euthanized. Tumors were excised,

weighed, photographed, and subjected to further histological and molecular analyses. For the lung metastasis model, 1×10^6 Luc-labeled HCC cells were injected into the tail vein of nude mice. Lung metastasis was monitored weekly using an in *vivo* bioluminescence imaging system (IVIS Spectrum, PerkinElmer). At the endpoint, lungs were harvested, fixed, and stained with hematoxylin and eosin (H&E) to assess metastatic burden. All procedures were performed under sterile conditions. Mice were housed in a specific pathogen-free (SPF) facility with ad libitum access to food and water.

Measurement of ECAR and OCR

The extracellular acidification rate (ECAR) and oxygen consumption rate (OCR) were measured using the Seahorse XF Analyzer (Agilent Technologies, USA) according to the manufacturer's instructions. HCC cells were seeded in Seahorse XF 96-well microplates and incubated overnight. For ECAR measurements, the Glycolysis Stress Test Kit was used; for OCR, the Mito Stress Test Kit was applied. Data were normalized to cell number or protein concentration, and results were analyzed using Wave software (Agilent).

Statistical Analysis

All data are presented as mean ± standard deviation (SD) from at least three independent experiments. Statistical analyses were performed using GraphPad Prism 8.0 software. Differences between two groups were assessed using the two-tailed Student's t-test, while comparisons among multiple groups were conducted using one-way ANOVA

followed by Tukey's post hoc test. Kaplan-Meier survival curves were analyzed using the log-rank test. A p-value < 0.05 was considered statistically significant.

Results

Upregulated METTL15 predicts poor prognosis in HCC

Analysis of The Cancer Genome Atlas Liver Hepatocellular Carcinoma (TCGA-LIHC) dataset revealed that METTL15 is highly expressed in hepatocellular carcinoma (HCC), and its expression level is significantly associated with tumor stage and grade (**Figure 1A and 1H**). Consistently, data from the Gene Expression Omnibus (GEO) database also demonstrated a marked upregulation of METTL15 expression in HCC tissues (**Figure 1B, 1C and 1D**). To further validate these findings, we collected tumor and adjacent non-tumor tissues from clinically confirmed HCC patients at Yongzhou Central Hospital, and assessed METTL15 expression using qPCR, Western blotting, and immunohistochemistry (**Figure 1E, 1F and 1G**). Kaplan-Meier survival analysis based on the TCGA dataset indicated that elevated METTL15 expression was significantly correlated with reduced overall survival in HCC patients (**Figure 1I**). Additionally, METTL15 expression was found to be notably higher in several HCC cell lines (Hep3B, Huh7, PLC5, and HCC-LM3) compared to normal liver cells (THLE-2) (**Figure 1J, 1K**). Based on these observations, we established stable METTL15 knockout and overexpression cell lines in Hep3B and Huh7 cells, with successful modulation confirmed by Western blot analysis (**Figure 1L**). RNA sequencing followed by KEGG pathway enrichment analysis revealed that METTL15 deficiency significantly perturbed mitochondrial metabolism and glycolysis-related pathways (**Figure 1M**). Collectively, these findings suggest that METTL15 may play a crucial role in HCC progression and holds potential as a diagnostic and prognostic biomarker for HCC.

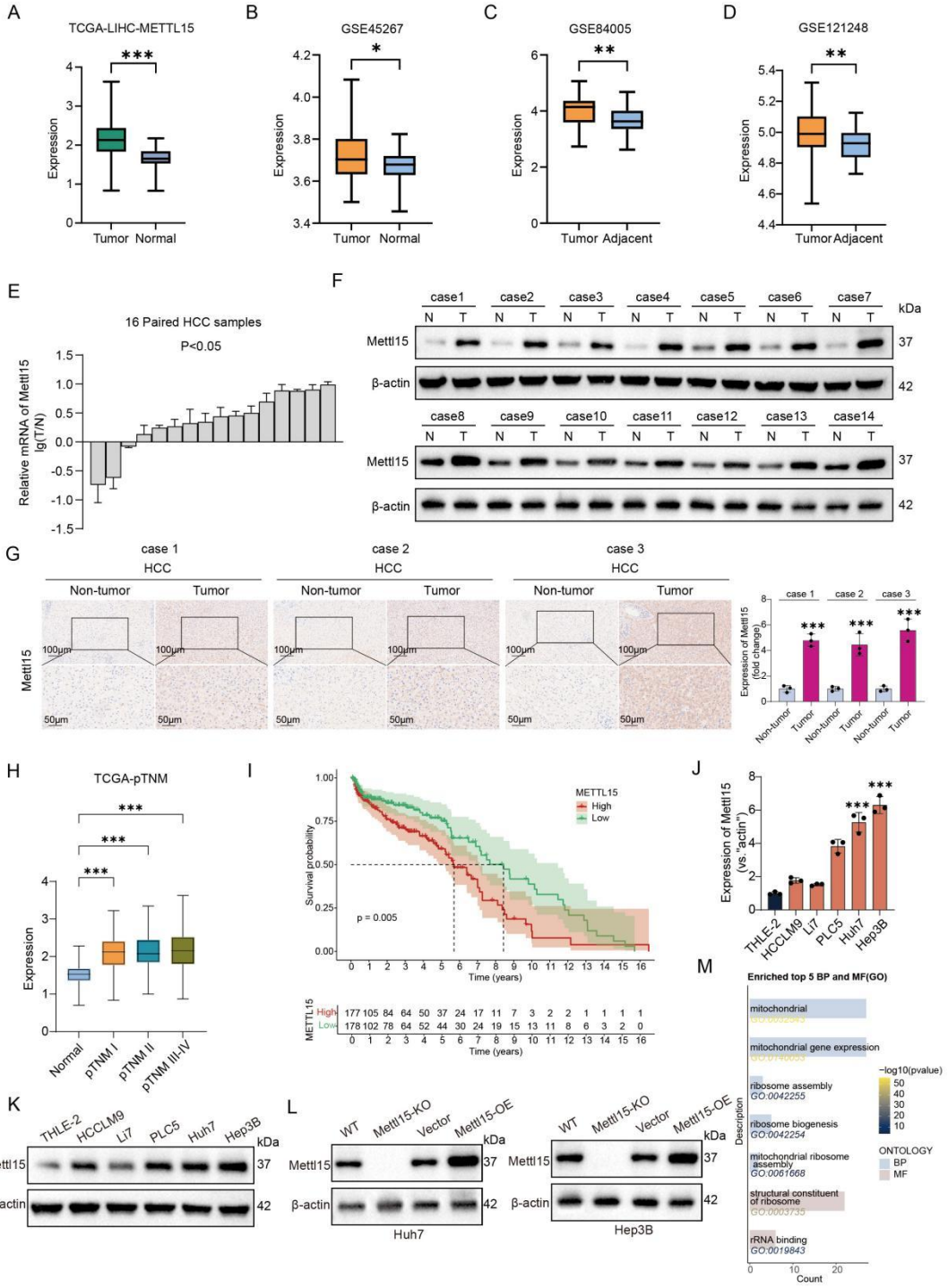


Figure 1. Up-regulation of METTL15 in HCC correlates with poor prognosis.

(A-B) METTL15 expression in normal tissues and HCC tissues from TCGA and GEO databases. **(C-D)** METTL15 expression in adjacent non-tumor tissues and HCC tissues from the GEO database. **(E)** qPCR analysis of METTL15 expression in 16 paired HCC

tumors and adjacent tissues. **(F)** METTL15 protein expression levels in 14 pairs of tumor and adjacent non-tumor tissues (n = 14 per group). **(G)** IHC staining and quantitative analysis of METTL15 in three representative HCC tissue samples. **(H)** METTL15 expression in HCC tissues stratified by pathological stage (I-IV) based on TCGA data. **(I)** Kaplan-Meier curves showing overall survival rates and the number of surviving patients stratified by METTL15 expression levels. **(J-K)** qPCR and WB analysis of METTL15 expression in immortalized hepatocytes and HCC cell lines, including THEL-2, HCCLM9, Li7, PLC5, Huh7 and Hep3B. **(L)** WB validation of METTL15 KO and OE efficiency in Huh7 and Hep3B cell lines. **(M)** GO enrichment analysis of biological processes (BP) and molecular functions (MF) associated with METTL15.

METTL15 promotes the proliferation and migration of HCC cells in *vitro*

To evaluate the role of METTL15 in the biological behavior of HCC cells, a series of in *vitro* functional assays were performed. CCK-8 and colony formation assays demonstrated that METTL15 overexpression significantly enhanced the proliferative capacity and colony-forming ability of HCC cells, whereas METTL15 knockout markedly suppressed cell proliferation (**Figure 2A, 2B, 2C and 2D**). EdU incorporation assays further confirmed the promotive effect of METTL15 on DNA synthesis and cell proliferation (**Figure 2G and 2H**). Furthermore, transwell migration and wound healing assays revealed that METTL15 overexpression significantly promoted the migratory ability of HCC cells, while its depletion led to a notable reduction in cell migration (**Figure 2E, 2F, 2I and 2J**). Collectively, these findings suggest that METTL15 plays a crucial role in promoting the proliferation and migration of HCC cells.

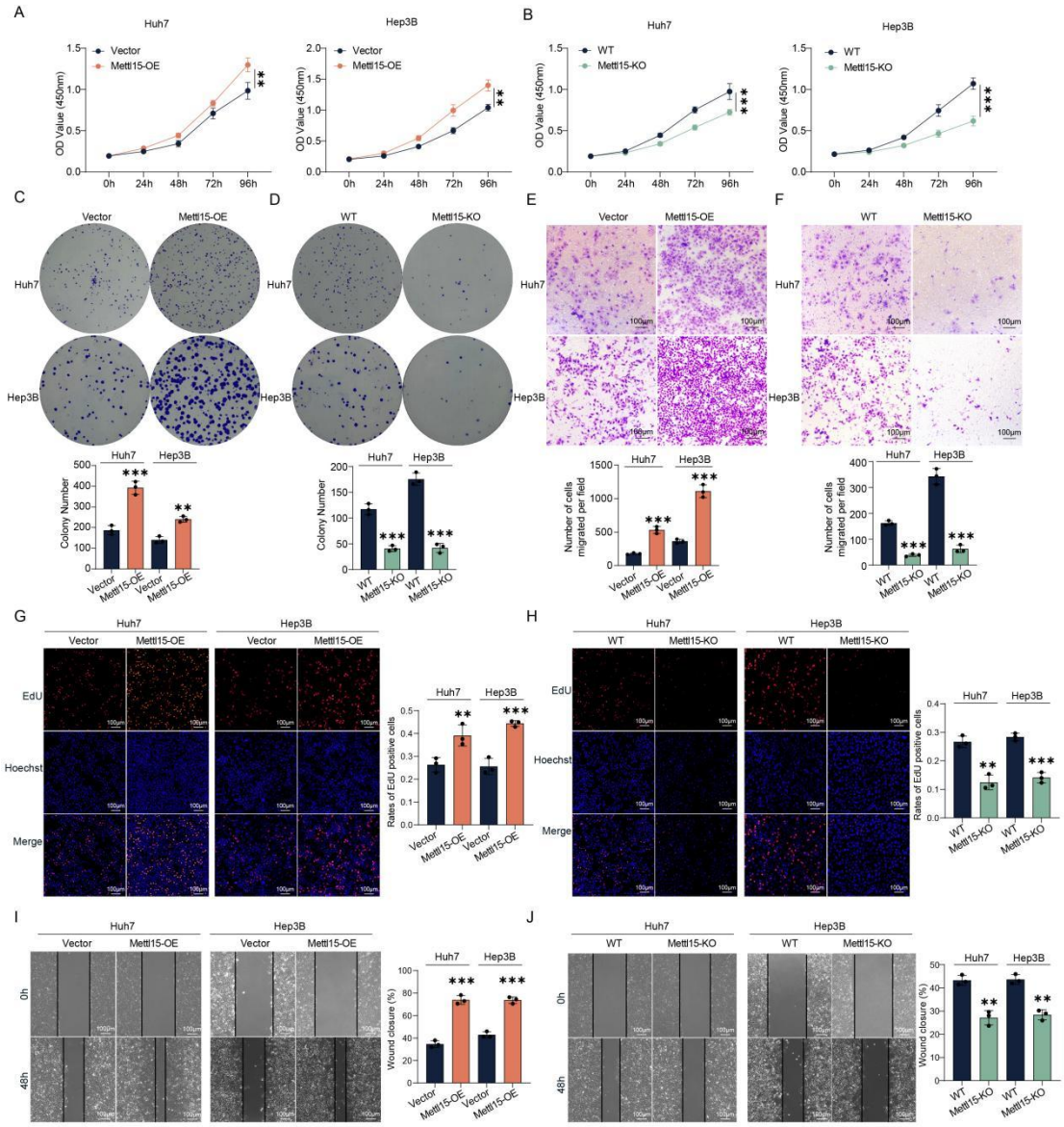


Figure 2. METTL15 promotes the proliferation, migration, and invasion of HCC cells in *vitro*.

(A-B) CCK8-based cell viability assays were conducted to assess how METTL15 overexpression or knockout affects the viability of Huh7 and Hep3B cell lines. **(C-D)** Colony formation experiments were performed to compare the colony-forming capacities of Huh7 and Hep3B cells with stable METTL15 overexpression or knockout. **(E-F)** Transwell migration assays were carried out to examine the migration ability of Huh7 and Hep3B cells following METTL15 overexpression or knockout (n = 3 per group). Scale bar, 100 μm, 10× magnification. **(G-H)** EdU assay was used to determine the proportion of proliferating cells in Huh7 and Hep3B after METTL15

overexpression or knockout (n = 3 per group). Scale bar, 100 μm, 10× magnification. **(I-J)** Scratch assay was employed to evaluate the migration ability of Huh7 and Hep3B cells after METTL15 overexpression or knockout (n = 3 per group). Scale bar, 100 μm, 10× magnification. All data are expressed as mean ± SEM, with n=3 for cell experiments. Statistical significance: *p < 0.05, **p < 0.01, ***p < 0.001, and ns. denotes no statistical significance.

METTL15 enhances glycolysis to promote HCC progression.

Aiming at verifying the function of METTL15 in glycolysis, we measured glucose uptake and lactate production, key indicators of glycolytic activity, in METTL15-knocked out or overexpressed cells. Under hypoxic conditions, we observed the glucose uptake capacity (**Figure 3A and 3E**), lactate production rate (**Figure 3B and 3F**), pyruvate production rate (**Figure 3C and 3G**), and cell viability (**Figure 3D and 3H**) in tumor cells following METTL15 knockout and overexpression, respectively. We observed that METTL15 knockout significantly reduced the glucose uptake capacity of tumor cells, accompanied by decreased lactate and pyruvate production rates, and a reduction in cell viability. In contrast, METTL15 overexpression significantly enhanced glucose uptake and glycolysis levels in HCC cells, with increased cell viability. Functional analysis showed that METTL15 overexpression led to an elevated extracellular acidification rate (ECAR) level(**Figure 3K**), whereas METTL15 knockout caused a significant decrease in ECAR (**Figure 3I**). METTL15 overexpression resulted in a decrease in oxygen consumption rate (OCR) (**Figure 3L**), while METTL15 knockout led to a significant increase in OCR (**Figure 3J**). Using mito-dsRed-labeled METTL15 knockout HCC cells, confocal microscopy revealed enhanced mitochondrial function, whereas METTL15 overexpression impaired mitochondrial function (**Figure 3M**). Measurement of glycolytic intermediates indicated that METTL15 overexpression increased the levels of glucose-6-phosphate, lactate, and other glycolytic intermediates. RNA and protein expression analyses showed that METTL15 knockout led to downregulation of glycolysis-related genes, such as HK2, 6-Phosphofructo-2-Kinase/Fructose-2,6-Bisphosphatase 3 (PFKFB3), Lactate

Dehydrogenase A (LDHA), Triosephosphate Isomerase 1 (TPI1), and PKM2, whereas METTL15 overexpression resulted in significant upregulation of these genes (**Figure 3N and 3O**).

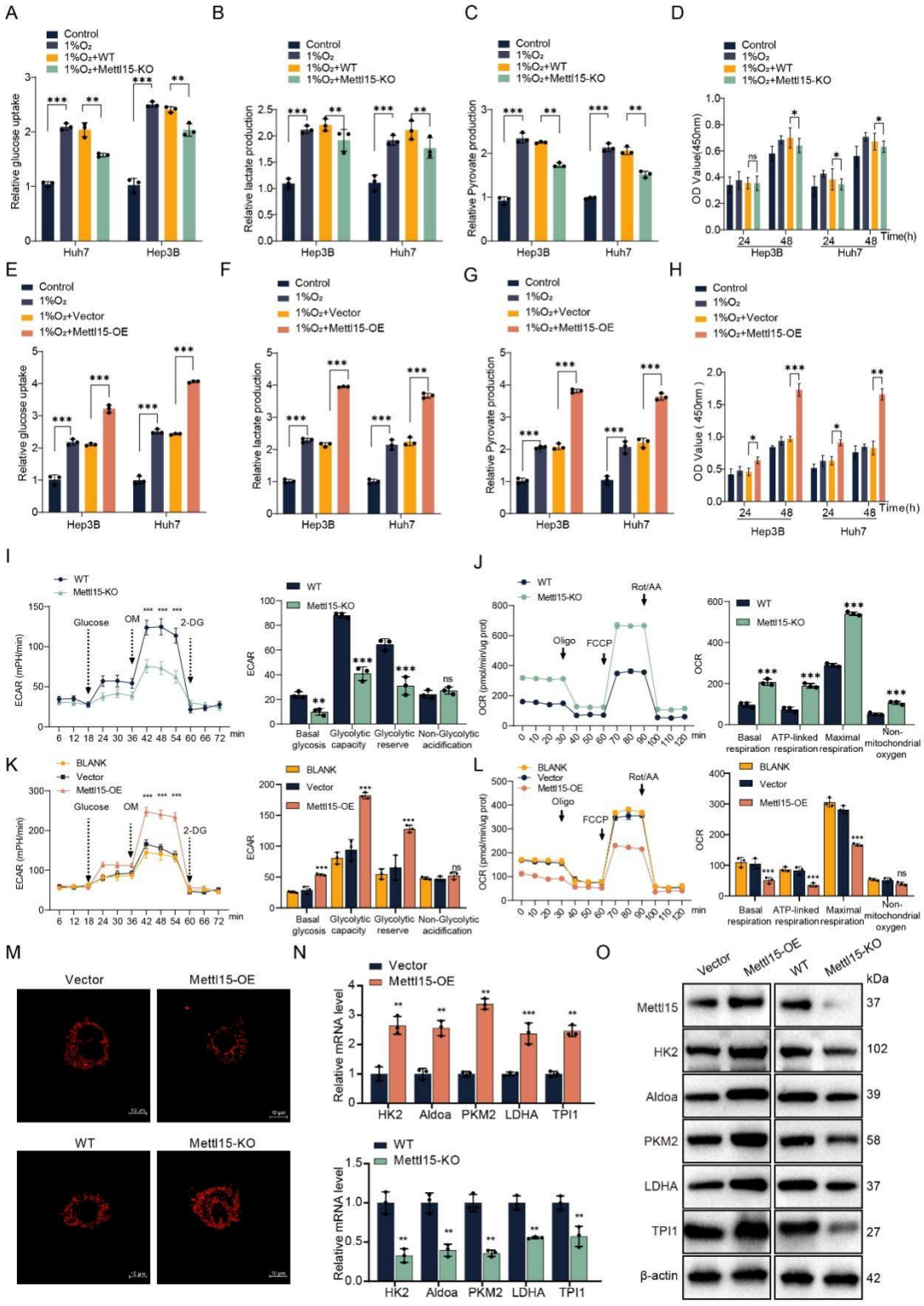


Figure 3. METTL15 enhances the Warburg effect in HCC cells.

(A) Measurement of glucose uptake in METTL15 knockout Huh7 and Hep3B cells under hypoxic conditions to assess the impact of METTL15 on HCC glycolysis. Glucose uptake was quantified using a glucose uptake assay kit. **(B)** Measurement of lactate production in the culture media of METTL15 knockout Huh7 and Hep3B cells under hypoxic conditions to assess the glycolytic effect of METTL15. Lactate levels were determined using a lactate assay kit. **(C)** Measurement of pyruvate levels using a colorimetric pyruvate assay kit in METTL15 knockout Huh7 and Hep3B cells to explore the role of METTL15 in glycolysis. **(D)** CCK-8 assays were performed to assess the metabolic activity and proliferation of METTL15 knockout Huh7 and Hep3B cells under hypoxic conditions, providing insight into the role of METTL15 in HCC cell growth and survival under glycolytic conditions. **(E-H)** Effects of METTL15 overexpression on glucose uptake, lactate production, pyruvate production, and cell viability in HCC cells. **(I-L)** Extracellular acidification rate (ECAR) levels in METTL15 knockout (I) and overexpression (K) Huh7 cell lines were measured to reflect METTL15's impact on glycolysis. Oxygen consumption rate (OCR) levels in METTL15 knockout (J) and overexpression (L) Huh7 cell lines were assessed to evaluate METTL15's impact on glycolysis in HCC cells. **(M)** Mitochondrial morphology and distribution in Huh7 cells treated with METTL15 overexpression or knockout were observed using confocal microscopy after transfection with a mito-dsRed-labeled virus. ImageJ software was used to quantify the mitochondrial fluorescence intensity, distribution, and morphology changes. **(N-O)** Expression of glycolysis-related genes was evaluated by qPCR and WB assays. Data are presented as mean ±SD, and statistical significance between groups was determined using Student's t-test: ***$p \leq 0.001$, **$p \leq 0.01$, *$0.01 < p \leq 0.05$, n.s. indicates no statistical significance.

METTL15 promotes in *vivo* growth and metastasis of HCC cells

To evaluate the effects of METTL15 on tumor proliferation and metastasis, in *vivo* animal experiments were performed. Wild-type (WT) and METTL15 knockout (METTL15-KO) HCC-Huh7 cells were subcutaneously injected into nude mice. Gross tumor images and growth curves revealed that tumor growth in the METTL15-KO group was markedly slower compared to the WT group (**Figure 4A**). Meanwhile, HCC-Huh7 cells with METTL15 overexpression (METTL15-OE) or empty vector (Vector) were also subcutaneously implanted into nude mice. The results showed that tumors in the METTL15-OE group grew significantly faster than those in the Vector group (**Figure 4B**). Bioluminescence imaging further demonstrated that the tumor signal intensity was significantly reduced in the METTL15-KO group compared to the WT group, while METTL15 overexpression markedly increased the tumor signal intensity compared to the control group (**Figure 4C and 4D**). Consistently, tumor weights were significantly affected by METTL15 expression levels (**Figure 4E**).

Subsequently, lactate and pyruvate levels in the subcutaneous tumor tissues were measured. METTL15 knockout led to a significant reduction in intratumoral lactate and pyruvate levels, while METTL15 overexpression resulted in elevated levels of these glycolytic metabolites (**Figure 4F**). To further investigate the role of METTL15 in metastasis, an experimental lung metastasis model was established by tail vein injection of Luc-labeled HCC-Huh7 cells (WT or METTL15-KO). The number and fluorescence intensity of lung metastatic nodules were significantly decreased in the METTL15-KO group (**Figure 4G**). Immunohistochemistry (IHC) analysis showed that METTL15 protein expression was markedly elevated in the METTL15-OE group compared to the Vector group. Ki-67 staining revealed a significant increase in proliferating cells in the METTL15-OE group. Moreover, the expression levels of key glycolytic enzymes HK2 and PKM2 were significantly upregulated in tumors from the METTL15-OE group (**Figure 4H**). Collectively, these findings suggest that METTL15 promotes tumor cell proliferation, glycolytic activity, and metastatic potential in *vivo*.

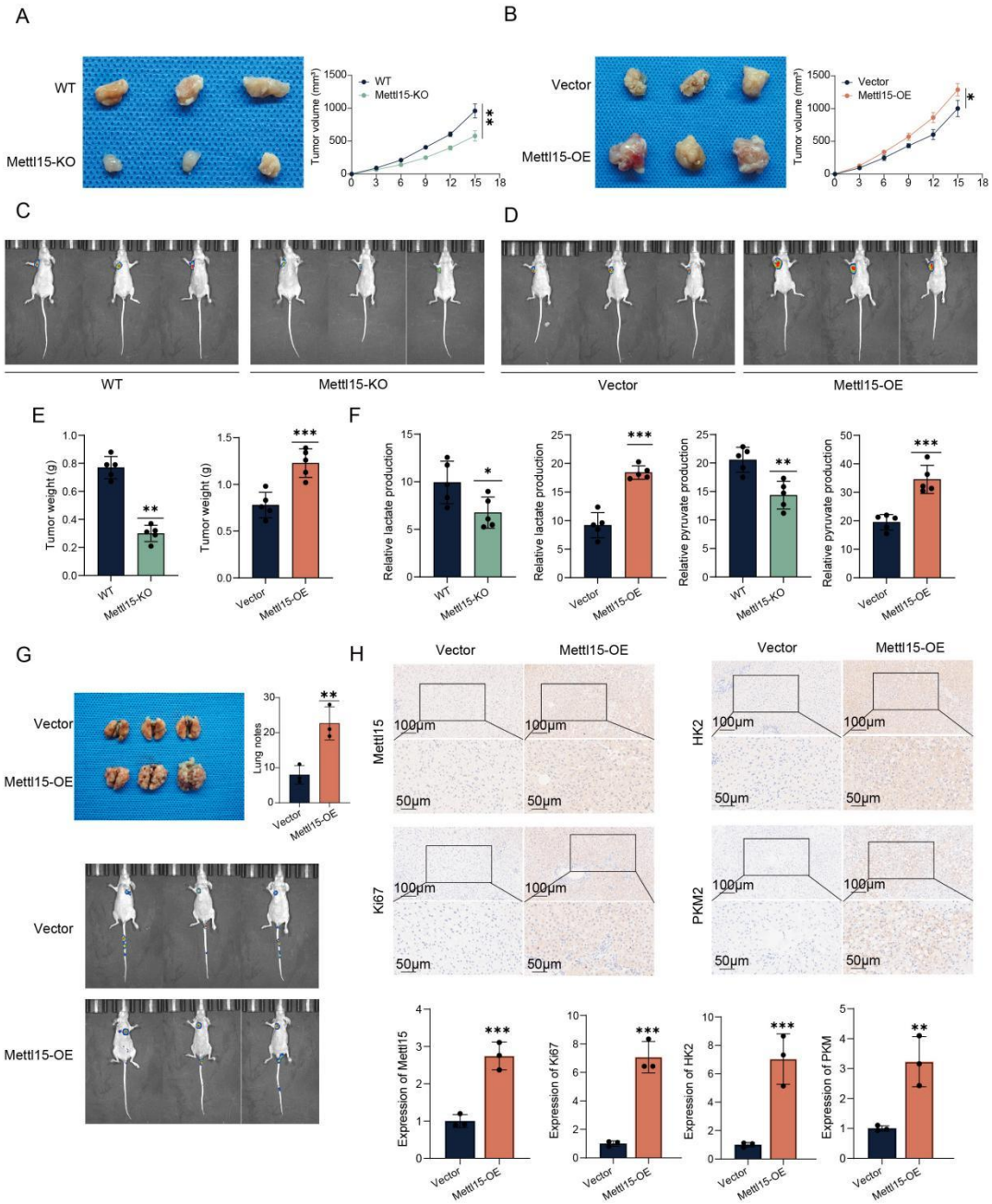


Figure 4. METTL15 promotes in *vivo* growth and metastasis of HCC cells。

(A-B) A xenograft model was established by subcutaneous injection of Huh7 cells into mice (METTL15 overexpression group and vector control group; METTL15 knockout group and NC control group). Tumor images and growth curves are presented. Tumor diameters were measured every four days using calipers (n=3 per group).**(C-D)** Regular in *vivo* imaging of the mice was performed using a small animal imaging system to

assess bioluminescent signal intensity of subcutaneous xenografts. **(E)** Tumor weights were measured using an electronic scale to assess the differences between the METTL15 overexpression group and vector control group, as well as the METTL15 knockout group and NC control group. **(F)** To evaluate the impact of METTL15 on tumor metabolism, lactate concentrations in the tumors from xenograft models were measured using a lactate assay kit; pyruvate concentrations were measured using a pyruvate assay kit. Tumor tissues were homogenized, and lactate or pyruvate content was detected following the manufacturer's instructions. **(G)** Quantification of lung metastatic nodes and bioluminescent signal intensity in an experimental lung metastasis model. **(H)** IHC analysis of METTL15, Ki-67, HK2, and PKM2 expression in xenograft tumors. All animal experiments were performed with at least 3 biological replicates. Data are presented as mean ± SD, and statistical significance between groups was determined using Student's t-test: ***$p \leq 0.001$, **$p \leq 0.01$, *$0.01 < p \leq 0.05$, n.s. indicates no statistical significance.

METTL15 regulates c-Myc expression by modulating the stability and translation of c-Myc mRNA

Glycolysis in cancer cells is regulated by several key transcription factors, among which c-Myc, P53, and HIF-1α are particularly prominent. In our study, we found that c-Myc expression was significantly downregulated upon METTL15 knockout, whereas its level was elevated in cells overexpressing METTL15 (**Figure 5A**). In contrast, the expression levels of P53 and HIF-1α remained unchanged (**Figure 5B and 5C**), suggesting that c-Myc may serve as a downstream effector of METTL15. To confirm this regulatory relationship, we first examined the transcriptional and translational stability of c-Myc following METTL15 depletion. Actinomycin D chase assays revealed that c-Myc mRNA exhibited a significantly increased decay rate in METTL15-knockout Hep3B and Huh-7 cells, indicating reduced transcript stability (**Figure 5D**). Given our previous KEGG pathway analysis, which implicated METTL15 in the

regulation of anaerobic glycolysis, we next evaluated glycolytic function by measuring glucose uptake, lactate production, and pyruvate levels under hypoxic conditions. As expected, HCC cells exhibited enhanced anaerobic glycolytic activity under hypoxia; however, this response was significantly impaired in METTL15-deficient cells. Notably, transient overexpression of c-Myc in METTL15-knockout cells restored glycolytic activity, rescuing the reduced glucose uptake and metabolite production (**Figure 5E, 5F, 5G and 5H**). To further assess functional consequences, CCK-8 assays were performed under hypoxic conditions. METTL15 knockout markedly reduced cell proliferation, whereas c-Myc overexpression reversed this suppression, restoring proliferative capacity (**Figure 6A**). Consistent with these observations, extracellular acidification rate (ECAR), a key indicator of anaerobic glycolysis driven by lactate secretion was significantly decreased in METTL15-deficient cells, but elevated upon c-Myc overexpression (**Figure 5I**). Furthermore, expression of anaerobic glycolysis-related genes at both the mRNA and protein levels was reduced following METTL15 knockout and subsequently restored by c-Myc reintroduction (**Figure 5L**). Together, these findings suggest that METTL15 promotes hypoxia-induced anaerobic glycolysis and cell proliferation in HCC cells, at least in part via stabilization and upregulation of c-Myc.

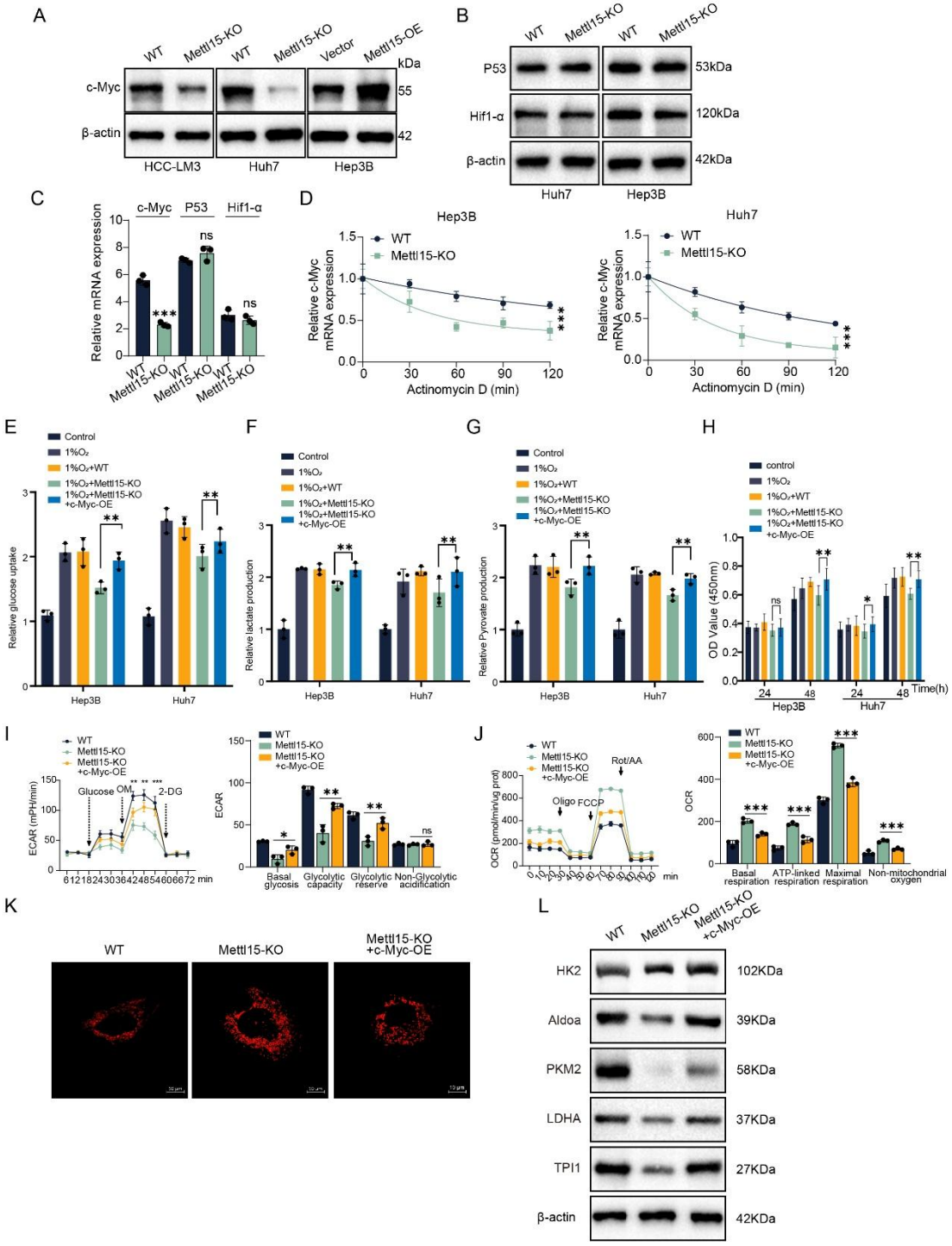


Figure 5. METTL15 regulates c-Myc expression by modulating the stability and translation of c-Myc mRNA.

(A-C) WB and qPCR analysis of c-Myc protein and mRNA levels in HCC cells under indicated treatments. **(D)** Effect of METTL15 KO combined with Actinomycin D

treatment on c-Myc mRNA stability, as determined by qPCR analysis. **(E-H)** Effects of indicated treatments on glucose uptake, lactate production, pyruvate production, and cell viability in HCC cells from the control, METTL15 knockout, and METTL15 knockout + c-Myc overexpressing groups. **(I-J)** ECAR and OCR in HCC cells treated as indicated, assessed using the Seahorse XFp Flux Analyzer. **(K)** Mitochondrial fluorescence staining of HCC cells from the control, METTL15 knockout, and METTL15 knockout + c-Myc overexpressing groups. **(L)** WB analysis of anaerobic glycolysis-related genes expression in HCC cells from the control, METTL15 knockout, and METTL15 knockout + c-Myc overexpressing groups. Data are presented as mean ± SD, and statistical significance between groups was determined using Student's t-test: ***$p \leq 0.001$, **$p \leq 0.01$, *$0.01 < p \leq 0.05$, n.s. indicates no statistical significance.

METTL15 promotes the growth and metastasis of HCC through c-Myc

To further investigate whether c-Myc is involved in METTL15-mediated tumor proliferation and metastasis, rescue experiments were conducted. CCK-8 and colony formation assays revealed that overexpression of c-Myc reversed the inhibitory effects of METTL15 knockout on cell proliferation (**Figure 6A, 6B and Figure S1A**). Similarly, transwell assays demonstrated that c-Myc overexpression restored the impaired migratory capacity caused by METTL15 deficiency in HCC cells (**Figure 6C and Figure S1B**). In addition, EdU incorporation assays showed that c-Myc overexpression rescued the reduction in proliferative activity induced by METTL15 knockout (**Figure 6D and Figure S1C**). Wound healing assays further confirmed that the attenuated migratory ability of HCC cells following METTL15 deletion was significantly reversed by c-Myc overexpression (**Figure 6E and Figure S1D**). In *vivo*, xenograft tumor models in nude mice showed that c-Myc overexpression partially rescued the suppressed tumor growth caused by METTL15 knockout (**Figure 6F, 6G and 6H**). Measurements of intratumoral pyruvate and lactate levels indicated that c-Myc overexpression reversed the reduction in glycolytic metabolites induced by

METTL15 deletion (**Figure 6I**). Immunohistochemical analysis further demonstrated that c-Myc overexpression counteracted the effects of METTL15 deficiency on tumor cell proliferation and glycolytic metabolism in *vivo* (**Figure 6J**). Figure 7 is a schematic diagram illustrating the mechanism by which METTL15 promotes the expression of c-Myc through an m^4C-dependent regulatory mechanism. Collectively, these findings strongly suggest that c-Myc acts as a downstream effector of METTL15 to promote tumor progression.

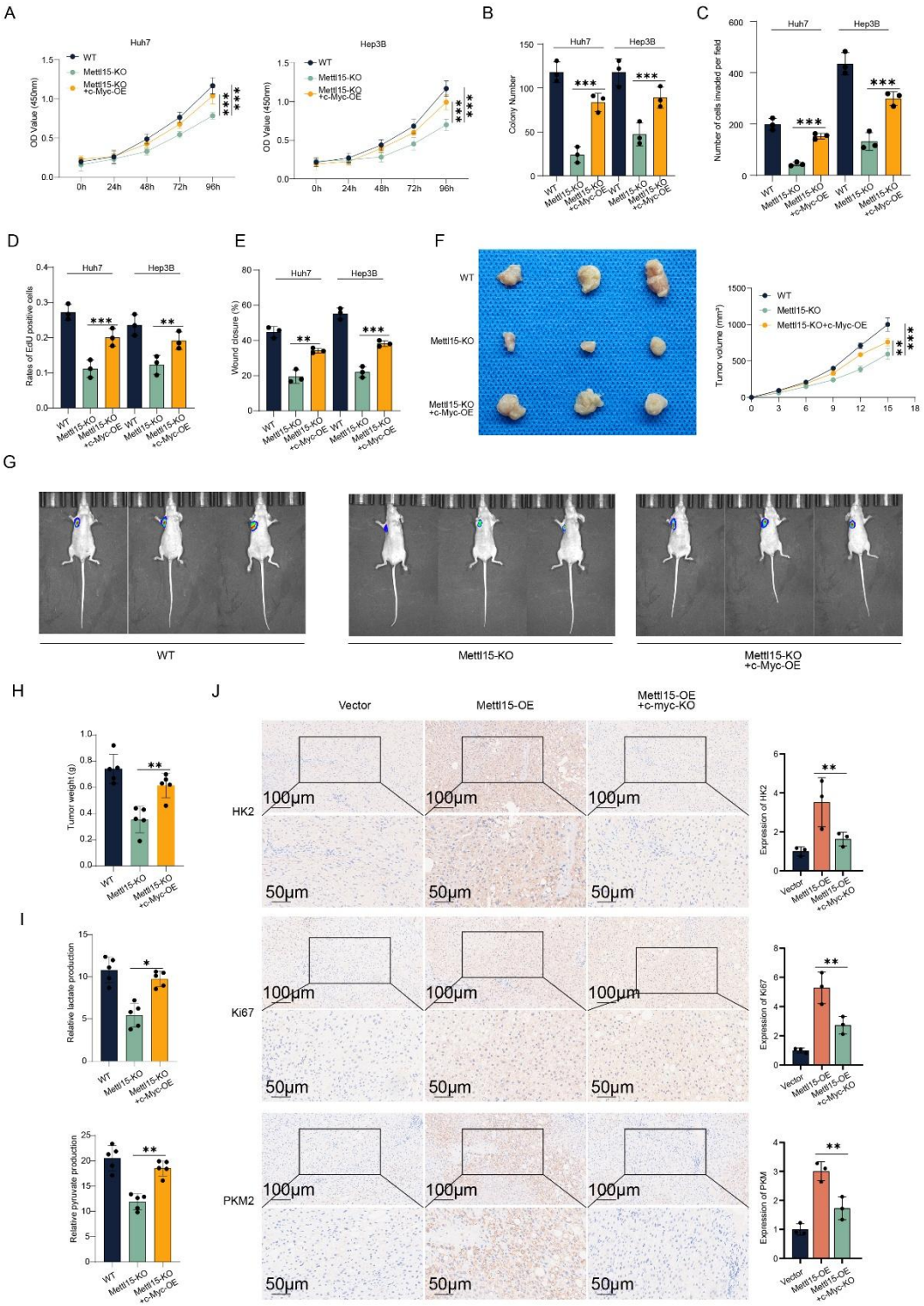


Figure 6. METTL15 promotes the growth and metastasis of HCC through c-Myc.

(A) CCK8-based cell viability assays were conducted to assess the effects of overexpression of c-Myc reversed the inhibitory effects of METTL15 knockout on the viability of Huh7 and Hep3B cell lines. **(B)** Colony formation experiments were

performed to compare the colony-forming capacities of Huh7 and Hep3B cells to assess the effects of overexpression of c-Myc reversed the inhibitory effects of METTL15 knockout. **(C)** Cell migration capacity was evaluated by Transwell migration assay performed in Hep3B and Huh7 cells from the control, METTL15 knockout, and METTL15 knockout + c-Myc overexpressing groups. **(D)** DNA synthesis and cell proliferation were analyzed by EdU assay performed in Hep3B and Huh7 cells from the control, METTL15 knockout, and METTL15 knockout + c-Myc overexpressing groups. **(E)** Cell migration was evaluated by wound healing assay performed in Hep3B and Huh7 cells from the control, METTL15 knockout, and METTL15 knockout + c-Myc overexpressing groups. **(F-H)** Volume and growth of subcutaneous xenografts of HCC-Huh7 cells. **(G)** Bioluminescent signal intensity of subcutaneous xenografts. **(H)** Tumor volume in xenograft models: Subcutaneous injection of Huh7 cells from the control, METTL15 knockout, and METTL15 knockout + c-Myc overexpressing groups. **(I)** Lactate and pyruvate levels in subcutaneous tumor tissues from the control, METTL15 knockout, and METTL15 knockout + c-Myc overexpressing groups. **(J)** Representative IHC staining images of HK2, Ki67, and PKM2 in tumor sections from the control, METTL15 overexpressing, and METTL15 overexpressing + c-Myc knockout groups.

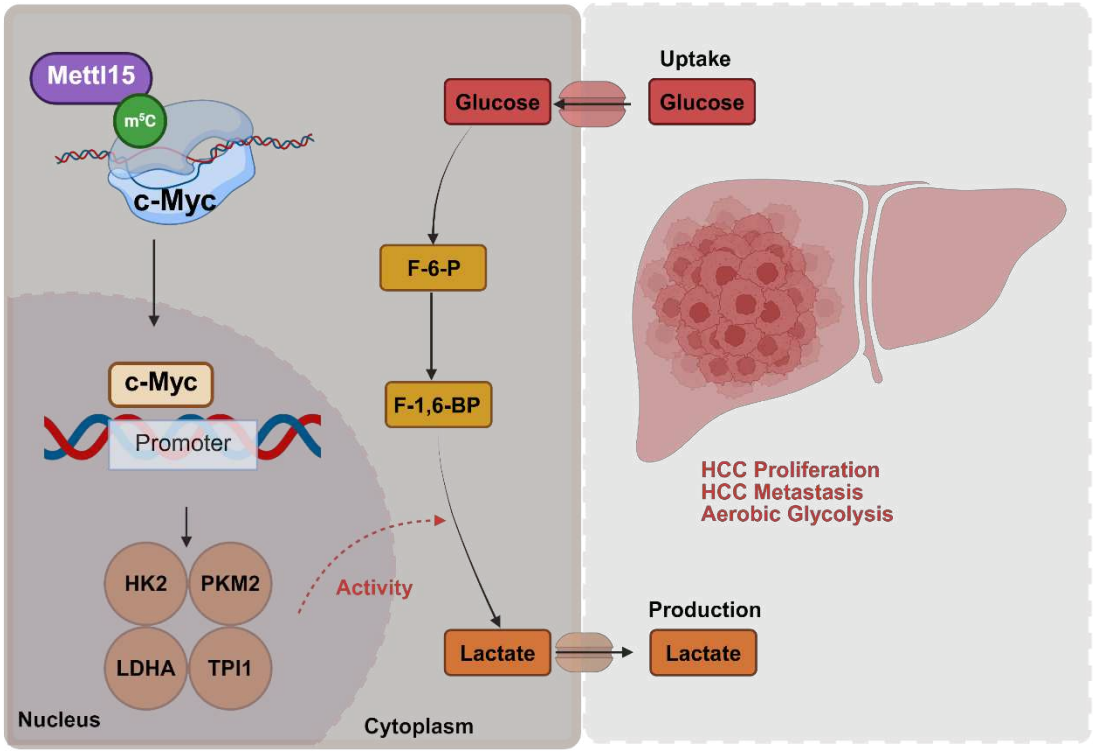


Figure 7. Schematic diagram illustrating that METTL15 promotes the expression of c-Myc through an m4C-dependent regulatory mechanism.

The schematic illustrates the central role of c-Myc in regulating key glycolytic enzymes. Upon transcriptional activation by c-Myc in the nucleus, enzymes including HK2, LDHA, PKM2, and TPI1 enhance glycolytic flux in the cytoplasm. This leads to increased glucose uptake and lactate production—a hallmark of aerobic glycolysis (the Warburg effect)—which fuels tumor growth, proliferation, and metastasis in gastric cancer.

Discussion

In this study, we identified METTL15 as a novel oncogenic driver in hepatocellular carcinoma (HCC), functioning through an epitranscriptomic mechanism to regulate glucose metabolic reprogramming. Our data demonstrate that METTL15 is markedly upregulated in HCC tissues and cell lines and that its high expression correlates with advanced tumor stage, poor differentiation, and unfavorable clinical prognosis.

Functionally, METTL15 enhances HCC cell proliferation, migration, and invasion, both in vitro and in vivo, thereby promoting tumor progression.

Mechanistically, we discovered that METTL15 promotes glycolytic metabolism by facilitating the translation of the proto-oncogene c-Myc in an m4C-dependent manner. METTL15 depletion led to reduced c-Myc protein levels without altering mRNA expression, suggesting a post-transcriptional regulatory mechanism. Moreover, actinomycin D chase assays confirmed decreased c-Myc mRNA stability following METTL15 knockout, highlighting a novel regulatory axis by which METTL15 may control key glycolytic regulators at the translational level.

Rescue experiments further corroborated the functional significance of c-Myc as a downstream effector of METTL15. Overexpression of c-Myc effectively restored the proliferative and migratory capacities of METTL15-deficient HCC cells and reversed the associated suppression of glycolytic activity. These findings not only underscore the pivotal role of METTL15 in driving metabolic adaptation via c-Myc but also highlight the therapeutic potential of targeting the METTL15-c-Myc axis in HCC.

Importantly, the metabolic reprogramming induced by METTL15 overexpression was characterized by enhanced glycolytic flux, increased extracellular acidification, and suppressed oxidative phosphorylation, resembling the Warburg effect. These alterations provide a metabolic advantage to tumor cells under hypoxic conditions and may contribute to resistance against conventional therapies.

Collectively, our findings establish METTL15 as a critical regulator of c-Myc-mediated glycolytic reprogramming and tumor progression in HCC. This study not only broadens

our understanding of RNA modification in cancer metabolism but also identifies METTL15 as a promising epitranscriptomic target for the development of novel therapeutic strategies in hepatocellular carcinoma.

Abbreviations

HCC: Hepatocellular Carcinoma, HK2: Hexokinase 2, PKM2: Pyruvate Kinase M2, LDHA: Lactate dehydrogenase A, m4C: N4-methylcytidine, TCGA: The Cancer Genome Atlas, LIHC: Liver Hepatocellular Carcinoma, GEO: The Gene Expression Omnibus, DEGs: Differentially expressed genes, DMEM: Dulbecco's Modified Eagle Medium, FBS: Fetal Bovine Serum, STR: Short tandem repeat, qRT-PCR: Quantitative Real-Time PCR, sgRNAs: Single guide RNAs, ECAR: Extracellular acidification rate, OCR: Oxygen consumption rate, PFKFB3: 6-Phosphofructo-2-Kinase/Fructose-2,6-Bisphosphatase 3, TPI1: Triosephosphate Isomerase 1, IHC: Immunohistochemistry.

Data Availability

Complete data will be accessible upon reasonable request from the corresponding author.

Author Contributions

Longhui Xie, Zhengsheng Ouyang and Changbin Pan conceived and coordinated the project. Yang Yang supervised the project. Changbin Pan and Lijuan Lv collected clinical HCC samples. Longhui Xie, Shaofei Xiao and Yang Yang performed most of the experiments. Changbin Pan and Jining Zeng analyzed the data. Yang Yang provided significant intellectual input. Longhui Xie wrote the manuscript with input

from all other authors. All authors reviewed and approved the final version of the manuscript to be submitted..

Funding

Funded by the Natural Science Foundation of Hunan Province, China (Grant No.2024JJ7580), the Natural Science Foundation of Hunan Province, China (Grant No.2023JJ50243) and the Shaoyang Science and Technology Project, China (Grant No. 2024PT4062).

Data sharing statement

All data are available in the main text or the Supplementary material.

Declaration of interests

The authors declare that they have no competing interests.

Acknowledgments

We express our gratitude to the teachers from the central Hospital of Yongzhou for their help in this study.

Ethics approval and consent to participate

This human-related study was approved by the Ethics Committee of the central Hospital of Yongzhou (permit number:2023110705). The tissue samples were obtained with written informed consent from each patient.

References

[1] Q. Dou, A.K. Grant, C. Callahan, P. Coutinho de Souza, D. Mwin, A.L. Booth, I. Nasser, M. Moussa, M. Ahmed, L.L. Tsai, PFKFB3-mediated Pro-glycolytic Shift in Hepatocellular Carcinoma Proliferation, Cellular and molecular gastroenterology and hepatology, 15 (2023) 61-75.

[2] K. Xu, J. Ding, L. Zhou, D. Li, J. Luo, W. Wang, M. Shang, B. Lin, L. Zhou, S. Zheng, SMYD2 Promotes Hepatocellular Carcinoma Progression by Reprogramming Glutamine Metabolism via c-Myc/GLS1 Axis, Cells, 12 (2022).

[3] D. Chen, A. Aierken, H. Li, R. Chen, L. Ren, K. Wang, Identification of subclusters and prognostic genes based on glycolysis/gluconeogenesis in hepatocellular carcinoma, Frontiers in immunology, 14 (2023) 1232390.

[4] C. Zhao, B. Wang, E. Liu, Z. Zhang, Loss of PTEN expression is associated with PI3K pathway-dependent metabolic reprogramming in hepatocellular carcinoma, Cell communication and signaling : CCS, 18 (2020) 131.

[5] M. Serra, M. Di Matteo, J. Serneels, R. Pal, S.T. Cafarello, M. Lanza, C. Sanchez-Martin, M. Evert, A. Castegna, D.F. Calvisi, M. Mazzone, A. Columbano, Deletion of Lactate Dehydrogenase-A Impairs Oncogene-Induced Mouse Hepatocellular Carcinoma Development, Cellular and molecular gastroenterology and hepatology, 14 (2022) 609-624.

[6] X. Ni, C.P. Lu, G.Q. Xu, J.J. Ma, Transcriptional regulation and post-translational modifications in the glycolytic pathway for targeted cancer therapy, Acta pharmacologica Sinica, 45 (2024) 1533-1555.

[7] M. Samec, A. Liskova, L. Koklesova, S.M. Samuel, K. Zhai, C. Buhrmann, E. Varghese, M. Abotaleb, T. Qaradakhi, A. Zulli, M. Kello, J. Mojzis, P. Zubor, T.K. Kwon, M. Shakibaei, D. Busselberg, G.R. Sarria, O. Golubnitschaja, P. Kubatka, Flavonoids against the Warburg phenotype-concepts of predictive, preventive and personalised medicine to cut the Gordian knot of cancer cell metabolism, The EPMA journal, 11 (2020) 377-398.

[8] K. Xu, N. Yin, M. Peng, E.G. Stamatiades, S. Chhangawala, A. Shyu, P. Li, X. Zhang, M.H. Do, K.J. Capistrano, C. Chou, C.S. Leslie, M.O. Li, Glycolytic ATP fuels phosphoinositide 3-kinase signaling to support effector T helper 17 cell responses, Immunity, 54 (2021) 976-987.e977.

[9] S. Paul, S. Ghosh, S. Kumar, Tumor glycolysis, an essential sweet tooth of tumor cells, Seminars in cancer biology, 86 (2022) 1216-1230.

[10] J.D. Bernstock, K.D. Kang, N.V. Klinger, H.E. Olsen, S. Gary, S.K. Totsch, G. Ghajar-Rahimi, D. Segar, E.M. Thompson, V. Darley-Usmar, B.T. Mott, L. Peruzzotti-Jametti, G.K. Friedman, Targeting oncometabolism to maximize immunotherapy in malignant brain tumors, Oncogene, 41 (2022) 2663-2671.

[11] R. Zhou, W. Ni, C. Qin, Y. Zhou, Y. Li, J. Huo, L. Bian, A. Zhou, J. Li, A functional loop between YTH domain family protein YTHDF3 mediated m(6)A modification and phosphofructokinase PFKL in glycolysis of hepatocellular carcinoma, Journal of experimental & clinical cancer research : CR, 41 (2022) 334.

[12] H. Tao, X. Zhong, A. Zeng, L. Song, Unveiling the veil of lactate in tumor-associated macrophages: a successful strategy for immunometabolic therapy, Frontiers in immunology, 14 (2023) 1208870.

[13] Y. Huang, Targeting glycolysis for cancer therapy using drug delivery systems, Journal of controlled release : official journal of the Controlled Release Society, 353 (2023) 650-662.
[14] H. Yu, J. Zhu, L. Chang, C. Liang, X. Li, W. Wang, 3-Bromopyruvate decreased kidney fibrosis and fibroblast activation by suppressing aerobic glycolysis in unilateral ureteral obstruction mice model, Life sciences, 272 (2021) 119206.
[15] J.N. Pak, H.J. Lee, D.Y. Sim, J.E. Park, C.H. Ahn, S.Y. Park, J.H. Khil, B. Shim, B. Kim, S.H. Kim, Anti-Warburg effect via generation of ROS and inhibition of PKM2/beta-catenin mediates apoptosis of lambertianic acid in prostate cancer cells, Phytotherapy research : PTR, 37 (2023) 4224-4235.
[16] C. Geng, L. Yan, Y. Li, H. Li, Y. Ji, Y. Xiao, Z. Wang, X. Chen, C. Chen, Q. Yang, B. Tang, W. Wang, Layered Double Hydroxide Nanoparticles Loaded with Resveratrol Inhibit Glycolysis and Show Efficacy in the Treatment of Breast Cancer, International journal of nanomedicine, 20 (2025) 3423-3444.
[17] Q. Qi, R. Zhong, Y. Huang, Y. Tang, X.W. Zhang, C. Liu, C.F. Gao, L. Zhou, J. Yu, L.Y. Wu, The RNA M5C methyltransferase NSUN2 promotes progression of hepatocellular carcinoma by enhancing PKM2-mediated glycolysis, Cell death & disease, 16 (2025) 82.
[18] G. Jia, Y. Wang, C. Lin, S. Lai, H. Dai, Z. Wang, L. Dai, H. Su, Y. Song, N. Zhang, Y. Feng, B. Tang, LNCAROD enhances hepatocellular carcinoma malignancy by activating glycolysis through induction of pyruvate kinase isoform PKM2, Journal of experimental & clinical cancer research : CR, 40 (2021) 299.
[19] C. Zhang, T. Yang, H. Chen, X. Ding, H. Chen, Z. Liang, Y. Zhao, S. Ma, X. Liu, METTL3 inhibition promotes radiosensitivity in hepatocellular carcinoma through regulation of SLC7A11 expression, Cell death & disease, 16 (2025) 9.
[20] Z. Zeng, J. Wang, F. Xu, P. Hu, Y. Hu, W. Zhuo, D. Chen, S. Han, F. Wang, Y. Zhao, Y. Huang, G. Zhao, The m6A modification-mediated positive feedback between glycolytic lncRNA SLC2A1-DT and c-Myc promotes tumorigenesis of hepatocellular carcinoma, International journal of biological sciences, 20 (2024) 1744-1762.
[21] L. Du, Y. Li, M. Kang, M. Feng, Y. Ren, H. Dai, Y. Wang, Y. Wang, B. Tang, USP48 Is Upregulated by Mettl14 to Attenuate Hepatocellular Carcinoma via Regulating SIRT6 Stabilization, Cancer research, 81 (2021) 3822-3834.
[22] H. Peng, B. Chen, W. Wei, S. Guo, H. Han, C. Yang, J. Ma, L. Wang, S. Peng, M. Kuang, S. Lin, N(6)-methyladenosine (m(6)A) in 18S rRNA promotes fatty acid metabolism and oncogenic transformation, Nature metabolism, 4 (2022) 1041-1054.
[23] M. Xue, L. Dong, H. Zhang, Y. Li, K. Qiu, Z. Zhao, M. Gao, L. Han, A.K.N. Chan, W. Li, K. Leung, K. Wang, S.P. Pokharel, Y. Qing, W. Liu, X. Wang, L. Ren, H. Bi, L. Yang, C. Shen, Z. Chen, L. Melstrom, H. Li, N. Timchenko, X. Deng, W. Huang, S.T. Rosen, J. Tian, L. Xu, J. Diao, C.W. Chen, J. Chen, B. Shen, H. Chen, R. Su, METTL16 promotes liver cancer stem cell self-renewal via controlling ribosome biogenesis and mRNA translation, J Hematol Oncol, 17 (2024) 7.
[24] Y.Z. Dai, Y.D. Liu, J. Li, M.T. Chen, M. Huang, F. Wang, Q.S. Yang, J.H. Yuan, S.H. Sun, METTL16 promotes hepatocellular carcinoma progression through downregulating RAB11B-AS1 in an m(6)A-dependent manner, Cellular & molecular biology letters, 27 (2022) 41.
[25] P. Xia, H. Zhang, H. Lu, K. Xu, X. Jiang, Y. Jiang, X. Gongye, Z. Chen, J. Liu, X. Chen, W. Ma, Z. Zhang, Y. Yuan, METTL5 stabilizes c-Myc by facilitating USP5 translation to

reprogram glucose metabolism and promote hepatocellular carcinoma progression, Cancer communications (London, England), 43 (2023) 338-364.
[26] Z. Chen, W. Zhu, S. Zhu, K. Sun, J. Liao, H. Liu, Z. Dai, H. Han, X. Ren, Q. Yang, S. Zheng, B. Peng, S. Peng, M. Kuang, S. Lin, METTL1 promotes hepatocarcinogenesis via m(7) G tRNA modification-dependent translation control, Clinical and translational medicine, 11 (2021) e661.
[27] F. Bi, Y. Qiu, Z. Wu, S. Liu, D. Zuo, Z. Huang, B. Li, Y. Yuan, Y. Niu, J. Qiu, METTL9-SLC7A11 axis promotes hepatocellular carcinoma progression through ferroptosis inhibition, Cell death discovery, 9 (2023) 428.
[28] X. Ye, J. Lin, Y. Chen, X. Wang, IGF2BP1 accelerates the aerobic glycolysis to boost its immune escape in hepatocellular carcinoma microenvironment, Frontiers in immunology, 15 (2024) 1480834.
[29] M. Lv, W. Zhou, Y. Hao, F. Li, H. Zhang, X. Yao, Y. Shi, L. Zhang, Structural insights into the specific recognition of mitochondrial ribosome-binding factor hsRBFA and 12 S rRNA by methyltransferase METTL15, Cell discovery, 10 (2024) 11.
[30] H.Y. Lee, H.T. Nga, J. Tian, H.S. Yi, Mitochondrial Metabolic Signatures in Hepatocellular Carcinoma, Cells, 10 (2021).
[31] H. Chen, S. Gao, W. Liu, C.C. Wong, J. Wu, J. Wu, D. Liu, H. Gou, W. Kang, J. Zhai, C. Li, H. Su, S. Wang, F. Soares, J. Han, H.H. He, J. Yu, RNA N(6)-Methyladenosine Methyltransferase METTL3 Facilitates Colorectal Cancer by Activating the m(6)A-GLUT1-mTORC1 Axis and Is a Therapeutic Target, Gastroenterology, 160 (2021) 1284-1300.e1216.
[32] M. Li, A. Zhang, X. Qi, R. Yu, J. Li, A novel inhibitor of PGK1 suppresses the aerobic glycolysis and proliferation of hepatocellular carcinoma, Biomedicine & pharmacotherapy = Biomedecine & pharmacotherapie, 158 (2023) 114115.
[33] F. Wang, Y. Hu, H. Wang, P. Hu, H. Xiong, Z. Zeng, S. Han, D. Wang, J. Wang, Y. Zhao, Y. Huang, W. Zhuo, G. Lv, G. Zhao, LncRNA FTO-IT1 promotes glycolysis and progression of hepatocellular carcinoma through modulating FTO-mediated N6-methyladenosine modification on GLUT1 and PKM2, Journal of experimental & clinical cancer research : CR, 42 (2023) 267.
[34] T. Neuss, M.C. Chen, N. Wirges, S. Usluer, R. Oellinger, S. Lier, M. Dudek, T. Madl, M. Jastroch, K. Steiger, W. Schmitz, H. Einwachter, R.M. Schmid, Metabolic Reprogramming Is an Initial Step in Pancreatic Carcinogenesis That Can Be Targeted to Inhibit Acinar-to-Ductal Metaplasia, Cancer research, 84 (2024) 2297-2312.
[35] L. Zhao, N. Yu, Y. Zhai, Y. Yang, Y. Wang, Y. Yang, Z. Gong, Y. Zhang, X. Zhang, W. Guo, The ubiquitin-like protein UBTD1 promotes colorectal cancer progression by stabilizing c-Myc to upregulate glycolysis, Cell death & disease, 15 (2024) 502.
[36] T.C. Chan, Y.T. Chen, K.T. Tan, C.L. Wu, W.J. Wu, W.M. Li, J.M. Wang, Y.L. Shiue, C.F. Li, Biological significance of MYC and CEBPD coamplification in urothelial carcinoma: Multilayered genomic, transcriptional and posttranscriptional positive feedback loops enhance oncogenic glycolysis, Clinical and translational medicine, 11 (2021) e674.

Supplementary Files

This is a list of supplementary files associated with this preprint. Click to download.

- SupplementaryFigure.docx